Volume xx (200y), Number z, pp. 1–14

Modeling material microstructure using the Perlin noise function

F. Conde-Rodríguez[1], Á-.L. García-Fernández[1] and J.C. Torres[2]

[1]Departamento de Informática, University of Jaén, EPSJ, Campus las Lagunillas s/n, 23071, Jaén, Spain
[2]Departamento de Lenguajes y Sistemas Informáticos, ETSIIT, University of Granada, C/ Periodista Manuel Saucedo Aranda, s/n, 18071, Granada, Spain
fconde@ujaen.es, algarcia@ujaen.es, jctorres@ugr.es

Abstract

This paper introduces a precise and easy to use method for defining the microstructure of heterogeneous solids. This method is based on the concept of Heterogeneous Composite Bézier Hyperpatch, and allows to accurately represent the primary material proportions, as well as the size and shape of the material phases. The solid microstructure is modeled using two functions: a material distribution function (to compute the portion of the solid volume occupied by each primary material), and a modified Perlin noise function that determines the shape and size of each primary material phase.

With this method, the position and orientation of the solid in the modeling space $\mathbb{R}^3$ does not affect the portion of its volume that is occupied by each primary material, nor the shape and size of the phases. However, the solid microstructure is coherently and automatically modified when the shape of the solid is edited.

Regarding continuity, this method allows to define to which extent continuity (both in shape and material distribution) has to be preserved at the junction of the cells that compose the solid. This makes modeling geometrically complex figures very easy.

Keywords — *Heterogeneous solid modeling; Material microstructure; Heterogeneous composite Bézier hyperpatch*

CCS Concepts

• ***Computing methodologies*** → ***Volumetric models; Parametric curve and surface models; Modeling methodologies;*** *Continuous models;*

1. Introduction

Solids that are not made of a single material are called *heterogeneous*. Typically, the proportions of the different primary materials inside an heterogeneous solid vary throughout its volume, as shown in Figure 1.a). However, real-life solids usually consist of a mixture of small regions of the primary materials that have uniform physical and chemical properties. These regions are called *phases* [Tor02, JA06] (see Figure 1.b).

Although on a microscopic scale each phase is made of a single material and has homogeneous (isotropic) properties, the behaviour of an heterogeneous solid on a macroscopic scale depends on the size, number and distribution of the phases of each primary material. As a result, the physical and chemical properties of an heterogeneous solid vary throughout its volume [Tor02, BB07]. The term *microstructure* is used to refer to the way the material phases are organized inside the solid.

Heterogeneous solids are widely used in industry nowadays. The mix of materials they are made from and their internal microstructure make them show better physical and chemical properties than their constituent materials individually. This is due to the fact that properties like yield and tensile strength, ductility, fracture toughness, and creep and fatigue strength are *microstructure-sensitive*.

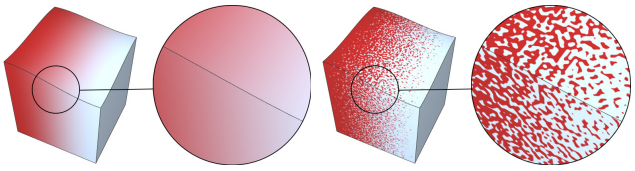

(a) Pure heterogeneous solid **(b)** Microstructure

Figure 1: Material at any point in ideal heterogeneous solids is a perfect mixture of the primary materials (a). However, real-life solids are not purely heterogeneous, they present microstructure instead. On a microscopic scale (b right), the solid is homogeneous (isotropic), as each phase is homogeneously composed of a single material; but on a macroscopic scale (b left) the solid has heterogeneous properties due to the spatial variation of the volume fraction of the phases.

Designing an heterogeneous solid and its internal microstructure is not an easy task. It is necessary to use a computer application based on a well stated framework in order to address all the complex aspects of the design process, including the size and shape of the material phases.

1.1. Main contributions of this paper

In [CTGF15, CRTGFFH17], a comprehensive framework based on Bézier hyperpatches that allows modeling heterogeneous solids in a simple and efficient way is described. The framework can automatically ensure continuity both in geometry and material distribution if needed. Section 2 summarizes the key concepts of the framework in order to make this paper self-contained.

- In this paper, we present an extension of the aforementioned framework to allow representing heterogeneous solid microstructures in a very controllable and accurate way. Here we describe a method to easily characterize and edit the internal microstructure of a solid that allows modeling different types of microstructures on different scales to fit many real manufacturing problems.
- We also describe how our microstructure modeling method allows to *automatically* preserve the continuity of the microstructure at the junction of the cells that compose the solid, if needed. It also allows modeling material discontinuities, as well as non-continuous junctions between cells. These features give the designer freedom to model geometrically complex pieces without having to worry about continuity issues.
- Moreover, we also highlight the fact that the shape, size and volume fraction of the phases inside the solid are not bound to their position and orientation in the modeling space $\mathbb{R}^3$. As a result, geometric deformations of an heterogeneous solid model do not affect its microstructure, and the modeling process becomes a quick, accurate and easy task.

1.2. Related work

The advances in additive manufacturing in the last years have boosted the interest in the development of representation models for heterogeneous materials. To gain insight regarding open problems about material structures, one can for example consult the paper [RRSS16] and its bibliography.

As stated previously, heterogeneous materials combine two or more primary materials in a microstructure. Such microstructures can be arranged in a regular pattern (a lattice, for example) or in a random way throughout the volume of the solid. The term *microarchitecture* is sometimes used to refer to regular microstructures [RRSS16], while keeping the term *microstructure* for the random ones (Figure 2). Note that the modeling method presented in this work only deals with random microstructures. For more details and interesting examples of microarchitecture modeling, one can review the papers [Elb17, ZSCM17, GAR18, ABC*19, WWG19, CRGFT20].

Regarding microstructure modeling, Bostanabad et al. published an interesting survey that covers a wide range of works dealing with microstructure characterization and reconstruction [BZL*18]. All the methods summarized in their survey propose different ways to characterize the material microstructure given a set of reference data (statistical data, reference images, physical descriptors, etcetera), and once this characterization has been obtained, they provide a method to simulate the microstructure over a given volume.

In [ST02], Siu and Tan discuss a solid modeling scheme that incorporates structure information such as dimension and orientation of fiber reinforcements within an heterogeneous solid model. They also develop a contour subdivision algorithm to discretize the material variation in each slice of the heterogeneous solid. Their modeling scheme applies to B-rep objects. In order to represent the material distribution inside the solid, they define a gradation function $f(d)$ that depends on the distance of the point that is evaluated to a reference datum named 'grading source'. This grading source can be a point, a line, a plane or the outermost boundaries of the model, and is fixed within the coordinate system of the model. This makes the gradation of materials within the model invariable when rigid transformations are applied, but it does not prevent the gradation of materials from changing when the model is deformed. In their work, Siu and Tan only consider 1D gradation.

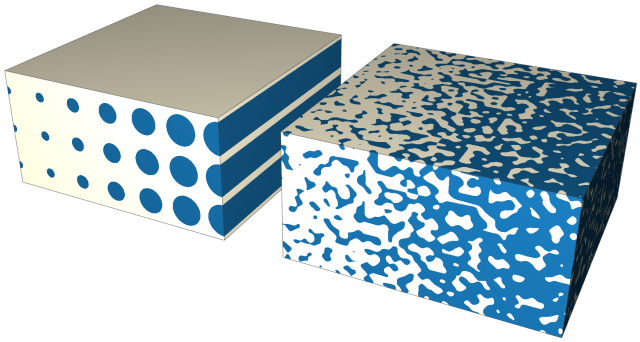

Figure 2: Left: heterogeneous solid with material microarchitecture. Right: heterogeneous solid with material microstructure

Massarwi et al. [ME16] propose a whole framework for volumetric object modeling based on trimmed B-spline trivariates that has a resemblance with ours. In their framework, an object is modeled through a *V-model*, which in turn is a set of disjoint *V-cells*. Each V-cell is bounded by *V-surfaces* and *V-curves*. Massarwi et al. present and discuss all the topology issues related with preserving a correct topological information of the model, as well as how to compute Boolean operations on V-models, and how to obtain a V-model from a B-rep model. Regarding material properties, instead of discussing microstructure representation, they propose to encode *attributes* as additional coordinates of the control points of the trivariates, or alternatively, define them as additional trivariates sharing the same parametric domain. Finally, they propose blending operations for calculating the new attribute values after a Boolean operation.

One of the usual working methodologies for generating microstructure models takes as input a series of images of the material to be simulated. This is the case of the proposal from Xu et al. [XDBC14], who study 2D images of the target material to characterize the microstructure in 2D through three features: composition, dispersion and geometry. Then, assuming that the material is isotropic and the phases are ellipsoids, they predict the feature values for the 3D microstructure, and propose an algorithm to reconstruct material microstructures similar to the input data. The method proposed by Liu and Shapiro [LS15] also takes as input a series of 2D images, and apply Markov Random Fields (MRF) to

generate microstructures, allowing to represent a great variety of random heterogeneous materials.

2D images are also the input data considered by Yang et al. [YNLS18]. The result of their processing of the images is a set of statistical descriptors of the material, as well as a shape library that stores the morphology of the material phases (either fibers or particles), parameterized as NURBS. This library is then used for creating the microstructure model: the phase models are sampled from the shape library, and the statistical descriptors are used to determine the amount of them to be generated. Finally, a packing algorithm and a genetic algorithm are applied to adjust the resulting microstructure, avoiding overlapping and ensuring that the result matches the statistical descriptors.

In [MDL16], Martínez et al. proposed an interesting method to directly model microstructures inspired by Voronoi open-cell foams, given a target elasticity value. Their method is inspired by the seminal work on cellular solid textures by Worley [Wor96], but it only applies to Voronoi-like microstructures. As an example, they apply the proposed method to the fabrication of objects with spatially varying elasticity.

Liu and Shapiro [LS18] presented a formal framework for modeling heterogeneous materials by recursive composition of two-scale material structures. This allows to maintain a dual material representation, so that depending on the scale (coarse or fine) of the operation to be computed, the more convenient representation is chosen (for example: a voxel-based representation on a coarse scale, and a Voronoi-based representation on a fine scale). They define upscaling and downscaling functions between the two representations based on neighbourhood functions, as well as how to compute the basic query functions of point membership classification, distance field query and material property across the two scales.

In their seminal paper [RT95], Roberts and Teubner define realistic random microstructures by defining the interface between two material phases through level cuts of gaussian random fields. This approach, commonly called random morphology description functions (RMDFs), is the most frequently used to simulate microstructures. It is also used by Vel and Goupee in [GV10, VG10], and more recently in [VCJG16] to model the solid domain in which properties of interest such as thermo elastic or thermo mechanical behaviour are calculated.

RMDFs are not intrinsically periodic, and therefore, preserving continuity between cells is a complex task. There are other types of functions more suitable for modeling continuity.

In [PFV*11], Pasko et al. describe a method to represent solids composed of a single material with internal microstructure, either regular or irregular. Their work is based on the FRep framework, and the material microstructure is represented using periodic functions. Regarding the problem that we address in this paper, Pasko et al. model irregular microstructures starting from regular microstructures and applying pseudo-random variations to the position and size of the pores.

Another related work is the one by Schmitt et al. [SPS04]. It presents a volume sculpting scheme based on CSG trees in which the primitives are trivariate B-Spline functions. For each solid, two independent trees are used: the first one is used for representing the geometry of the solid, while the second one is used for representing the material attributes. In order to edit the models, there are two independent sets of control points that allow controlling geometry and material separately. One of the advantages of this proposal is that set-theoretic operations are correctly supported for modeling purposes. On the other hand, in this and other methods for modeling microstructures via functional compositions, it might become difficult to relate the parameters of such functions to target material properties and/or descriptors [LS18].

2. Heterogeneous Composite Bézier Hyperpatches

In this section we summarize the key concepts of the framework in order to ease the understanding of the extensions we have made to it. A complete description of the framework can be found in [CTGF15]. In section 3 et seq. we explain how we have extended it to represent microstructure.

Definition 2.1 Material distribution
Let $\mathbf{M} = \{m_1, m_2, \ldots, m_n\}$ be a set of primary materials. Let $n = |\mathbf{M}|$ be the cardinality of $\mathbf{M}$. The *material distribution* of any given point $\mathbf{p}$ of an heterogeneous solid is represented by a tuple $\mathbf{a} = (a_1, a_2, \ldots, a_n) \in \mathbb{R}^n$, a_i being the volume fraction of material m_i at that point.

Not every possible material distribution is valid. In order for solids to be real, it is necessary that the volume fractions of the materials at any point in the solid are greater than or equal to 0 and add up to 1. Therefore, the valid space of material distributions $\mathbf{V}$ can be defined as:

$$\mathbf{V} = \left\{ \mathbf{a} \in \mathbb{R}^n \;\middle|\; \sum_{i=1}^{n} a_i = 1,\ a_i \geq 0 \right\} \tag{1}$$

A material distribution $\mathbf{a}$ is valid only if $\mathbf{a} \in \mathbf{V} \subseteq \mathbb{R}^n$; i.e., a material distribution is valid if its elements a_i are the coefficients of a convex combination of a set of primary materials $\mathbf{M}$.

If the set $\mathbf{M}$ of primary materials has only two materials $|\mathbf{M}| = 2$, a valid value of material distribution $\mathbf{a} = (a_1, a_2)$ can be written in a more convenient way as $\mathbf{a} = (a_1, 1 - a_1)$.

Definition 2.2 Heterogeneous Bézier hyperpatch
An heterogeneous Bézier hyperpatch $\mathbf{B}_m$ is defined by a function:

$$\mathbf{B}_m = \sum_{i=0}^{3}\sum_{j=0}^{3}\sum_{k=0}^{3} \mathbf{h}_{ijk} B_i^3(u) B_j^3(v) B_k^3(w); \quad u,v,w \in [0,1] \tag{2}$$

where B_i^3, B_j^3 and B_k^3 are the well-known Bézier blending functions, and $\mathbf{h}_{ijk} = (\mathbf{p}_{ijk}, \mathbf{a}_{ijk})$ are the heterogeneous geometric coefficients, which are pairs of values in which the elements

$$\mathbf{p}_{ijk} = (x_{ijk}, y_{ijk}, z_{ijk}) \in \mathbb{R}^3$$

are the points that define the shape of the hyperpatch (we will call them *geometric coefficients*), and the elements

$$\mathbf{a}_{ijk} = (a_{1_{ijk}}, a_{2_{ijk}}, \ldots, a_{n_{ijk}}) \in \mathbf{V} \subseteq \mathbb{R}^n$$

are the material distributions defining the gradation of the different materials throughout the hyperpatch.

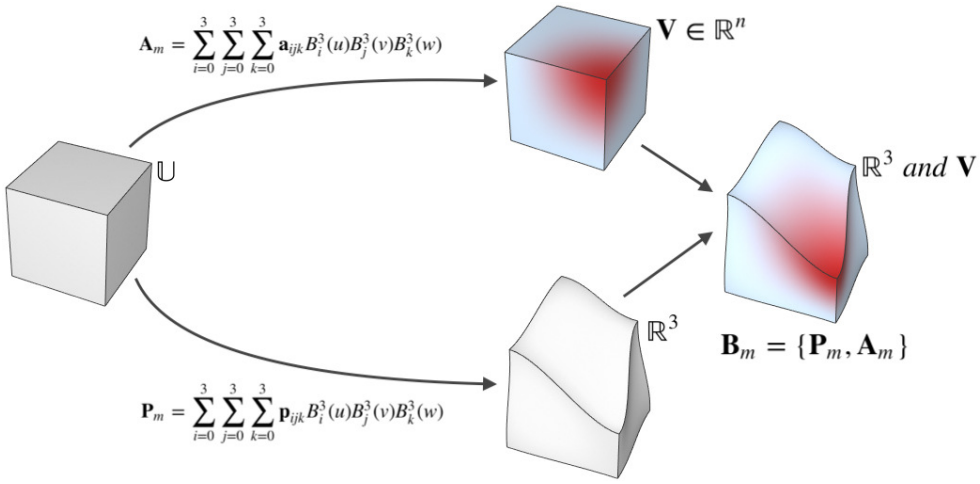

Figure 3: An heterogeneous Bézier hyperpatch $\mathbf{B}_m$ is defined by two functions. Function $\mathbf{P}_m$ defines its geometry, and function $\mathbf{A}_m$ defines the material distribution at every point

Therefore, an heterogeneous Bézier hyperpatch defines for every point (u,v,w) in the parametric domain $\mathbb{U}^3$ a 2-tuple consisting of a position in $\mathbb{R}^3$ and a material distribution at that position: $\mathbf{B}(u,v,w) = (\mathbf{P}(u,v,w), \mathbf{A}(u,v,w))$

Definition 2.3 Heterogeneous composite Béziér hyperpatch
An heterogeneous composite Bézier hyperpatch, $\mathbf{B}$, is a finite collection of heterogeneous Bézier hyperpatches.

$$\mathbf{B} = \{\mathbf{B}_1, \mathbf{B}_2, \ldots, \mathbf{B}_m\} \tag{3}$$

where $\mathbf{B}_i = (\mathbf{P}_i, \mathbf{A}_i)$. $\forall\ \mathbf{P}_i \in \mathbf{B}_i, \mathbf{P}_j \in \mathbf{B}_j\ \ i \neq j,\ \ \mathbf{P}_i \cap^* \mathbf{P}_j = \emptyset$. That is, the hyperpatches are pairwise disjoint, and at most, only share one, two or four corner points; one or four isoparametric boundary curves; and/or one isoparametric boundary surface.

In this framework, an heterogeneous solid is modeled by means of an heterogeneous composite Bézier hyperpatch i.e. by a cell decomposition in which each cell is an heterogeneous Bézier hyperpatch.

From now on, we are going to use either *parametric cell* or *hyperpatch* to refer to the heterogeneous Bézier hyperpatches in this decomposition. We are also going to use the term *composite hyperpatch* to refer to the whole heterogeneous solid.

From Equation 2, it can be inferred that a parametric cell $\mathbf{B}_m$ is defined by two functions:

$$\mathbf{B}_m = (\mathbf{P}_m, \mathbf{A}_m) \tag{4}$$

Function $\mathbf{P}_m$ defines the shape of the hyperpatch, and function $\mathbf{A}_m$ defines the gradation of the different materials throughout it.

$$\mathbf{P}_m = \sum_{i=0}^{3}\sum_{j=0}^{3}\sum_{k=0}^{3} \mathbf{p}_{ijk} B_i^3(u) B_j^3(v) B_k^3(w); \quad u,v,w \in [0,1] \tag{5}$$

$$\mathbf{A}_m = \sum_{i=0}^{3}\sum_{j=0}^{3}\sum_{k=0}^{3} \mathbf{a}_{ijk} B_i^3(u) B_j^3(v) B_k^3(w); \quad u,v,w \in [0,1] \tag{6}$$

Both functions are a parametric projection of a solid domain (a unit size cube, see Figure 3). The domain of the projection is known as *parametric space* $\mathbb{U}^3$, and the projection ranges are called *modeling space* $\mathbb{R}^3$ and *valid space of material distributions* $\mathbf{V}$ respectively.

That means that given a point of the solid denoted by $\mathbf{u} = (u,v,w) \in \mathbb{U}^3$, the hyperpatch function $\mathbf{B}_m$ returns two values: a point $\mathbf{p} = \mathbf{P}_m(u,v,w) \in \mathbb{R}^3$ indicating its position in three-dimensional space, and a material distribution $\mathbf{a} = \mathbf{A}_m(u,v,w) \in \mathbf{V} \subseteq \mathbb{R}^n$ indicating the proportion of each primary material at that point.

Composite hyperpatches accurately model their interior. It is possible to determine the material distribution $\mathbf{A}_m(\mathbf{u})$ and the position $\mathbf{P}_m(\mathbf{u})$ at every single point $\mathbf{u}$ of every single cell of the solid. In addition, the value obtained is a function of the parametric coordinates of each point.

This is very important, because the material distribution at any point of an heterogeneous solid modeled with our framework is not related to the current position of the solid in the modeling space $\mathbb{R}^3$, but to its coordinates in the parametric space $\mathbb{U}^3$, which do not change if we deform the solid (see Figure 3).

From Formula 2 one can also infer that the shape and material distribution of each parametric cell is determined by 64 heterogeneous geometric coefficients. Heterogeneous geometric coefficients of a parametric cell (see Figure 4.a) are organized in a three-dimensional array with indices i, j and k that vary from 0 to 3. In order to prevent editing operations on the geometric coefficients from producing non-valid (i.e. self-intersecting) solids, a validity condition [CRTC01] is imposed on the coefficients.

Not all coefficients have the same influence on the final shape or the material distribution of a parametric cell. We label as *corner points* the eight coefficients obtained by fixing the value of the three indices i, j and k, which take the value 0 or 3. They have the maximum influence both on the shape and the material distribution

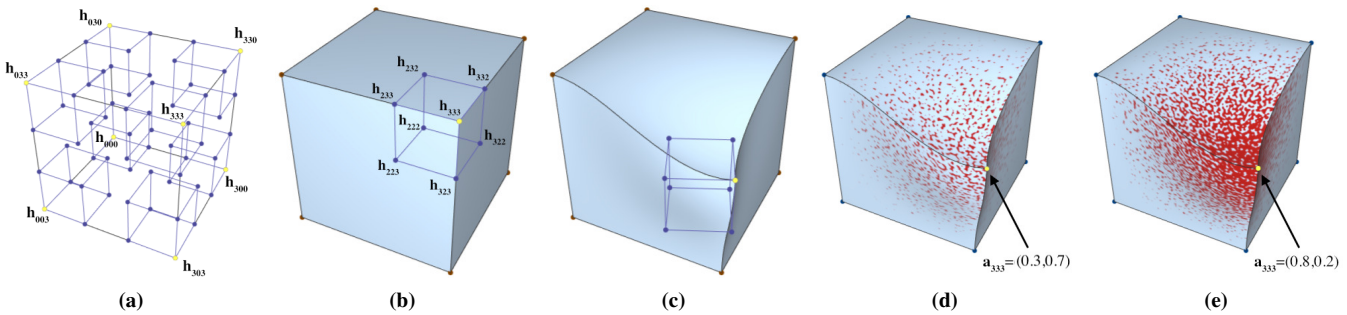

Figure 4: Heterogeneous geometric coefficients of an Heterogeneous Bézier Hyperpatch and their effect on material distribution and shape. (a) Array of 64 heterogeneous geometric coefficients. Only the eight corner points (in yellow) are labeled. (b) Each corner point (in yellow) and their immediate neighbours (in blue) have the strongest influence on the shape of the hyperpatch around that corner point. (c) Effect of moving and changing the orientation of the selected corner point. (d) An heterogeneous geometric coefficient is a pair that includes a material distribution. In this example $\mathbf{a_{333}} = (0.3, 0.7)$ while the material distributions of the other coefficients are equal to $\mathbf{a_{ijk}} = (0.0, 1.0)$ (e) Effect of changing the material distribution associated to the heterogeneous geometric coefficient $\mathbf{h_{333}}$ with respect to (d). The new material distribution is $\mathbf{a_{333}} = (0.8, 0.2)$

in each parametric cell, moreover, a hyperpatch always interpolate the corner points (see Figure 4).

There are several types of blending functions that can be used to combine heterogeneous geometric coefficients. We are using cubic Bézier blending functions $B_i^3(t)$:

$$B_0^3(t) = (1-t)^3 \qquad B_1^3(t) = 3t(1-t)^2 \tag{7}$$

$$B_2^3(t) = 3t^2(1-t) \qquad B_3^3(t) = t^3 \tag{8}$$

They were chosen for the following reasons:

- The glue conditions of two adjacent parametric cells expressed in Bézier form are much simpler to maintain automatically than if we use other functions like B-Spline. Therefore, Bézier blending functions facilitate modeling and editing complex real solids.
- Every Bézier hyperpatch interpolates its eight corner points, i.e. the hyperpatch passes through these points. Moreover, both the shape and the material distribution of each hyperpatch are determined by the positions and material distributions of its corner points. This greatly facilitates the edition of the composite hyperpatch. Especially when editing microstructure.
- The tangents to each corner point are defined by only its seven neighbouring geometric coefficients (in the array of 64 coefficients mentioned above). Thus, moving a control point close to a corner point have a clear effect on the shape of the hyperpatch around that corner point (see Figure 4.c.).

2.1. Continuity

Continuity is a very important property that has to be taken into account when creating and editing complex solids.

The surface tangent vectors at the corner points of a parametric cell depend exclusively on the geometric coefficients that surround each corner point. Taking into account the definition of a parametric cell and the distribution of the geometric coefficients described above and shown in Figure 4, the surface tangent vectors at the corner point $\mathbf{h}_{333}$ are determined by the geometric coefficients $\mathbf{h}_{323}$, $\mathbf{h}_{332}$, $\mathbf{h}_{322}$, $\mathbf{h}_{233}$, $\mathbf{h}_{223}$, $\mathbf{h}_{232}$ and $\mathbf{h}_{222}$ (shown in Figure 4.b).

Two adjacent parametric cells have C^1 continuity around a given shared corner point if each group of three neighbour geometric coefficients are collinear (see Figure 5.a.). Our framework allows to maintain C^1 continuity at the joint of the parametric cells by defining which geometric coefficients have to be moved in response to the edition of another one and how to compute their displacement (see Figures 5.b, 5.c and 5.d).

The condition of continuity for material distributions is slightly different. Given a material distribution $\mathbf{a}$ at a corner point shared by several parametric cells, we ensure C^1 continuity in the material distribution around that corner point by assigning the same material to all immediate neighbour coefficients in both parametric cells (see Figure 6). This is due to the fact that the material distributions are not elements of the set $\mathbb{R}^3$ but of the set $\mathbf{V} \in \mathbb{R}^n$, and $\mathbf{V}$ is not closed with respect to addition.

Both C^0 and C^1 continuity can be set independently for each corner point, and not all the four corner points of a boundary isosurface shared by two parametric cells have to be continuous or not continuous at the same time. Similarly, shape continuity at a given corner point can be activated independently from the material distribution continuity (see Figure 7).

Regarding C^2 continuity, the framework allows to ensure C^2 continuity in those parts of the solid that require it. This is accomplished by solving a linear equation that involves the corner points and its neighbour corner points. Nevertheless, as many authors state, *"... the usefulness of C^2 continuity is limited. Most mechanical parts do not require it, since fillets or rounded edges usually blend directly into face planes."* [Mor85] page 95.

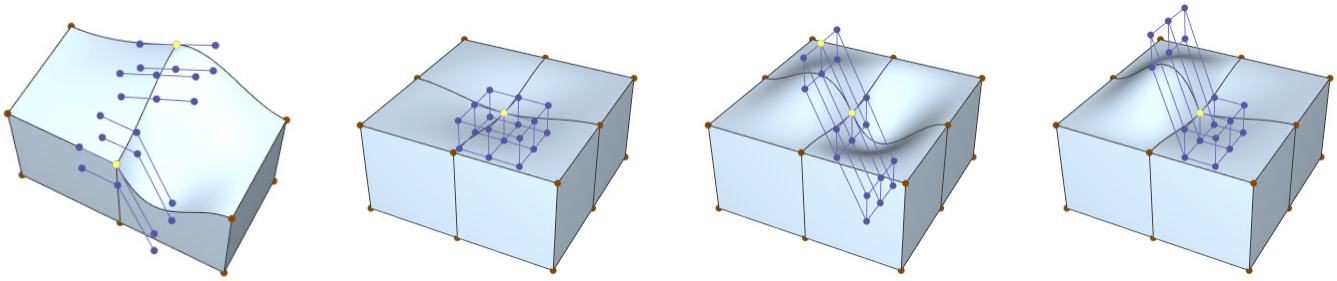

(a) (b) (c) (d)

Figure 5: Continuous / non continuous edition of the shape of a composite hyperpatch. (a) The corner points at the joint of two parametric cells (two of them are in yellow in the figure) are surrounded by four groups of three neighbour geometric coefficients. C^1 continuity is maintained if the geometric coefficients of each group are collinear (top part of the figure). (b) Composite hyperpatch to be edited. (c) Editing one of the neighbours (in yellow) of a corner point at the joint of four parametric cells with C^1 continuity activated results in a coordinated movement of the surrounding geometric coefficients to maintain continuity. (d) Result of moving several geometric coefficients with no continuity activated. The coefficients can be moved independently and the shape is modified accordingly.

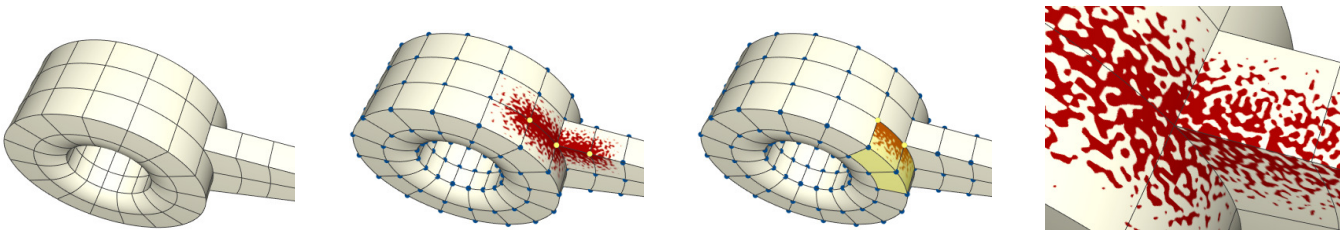

(a) (b) (c) (d)

Figure 6: Continuous / non continuous edition of the material distribution of a composite hyperpatch. (a) Composite hyperpatch to be edited. (b) Result of editing the material distribution at the corner points shared by several cells. The framework defines the appropriate corrections so that the microstructure extends continuously throughout the cells that share the corner points. (c) Result of a non continuous edition of the material distribution at the corner points shared by several cells. The framework defines how the effect is limited only to continuous adjacent cells. (d) Detailed view of the microstructure at the junction of the cells that share the corner points in (b). It can be seen that the material microstructure extends continuously across adjacent cells.

3. Modeling microstructure

Once the framework to model heterogeneous solids has been summarized, now we are going to focus on the contribution of this paper, which is the extension of this framework to define and represent material microstructures.

In order to characterize the microstructure of a solid, we use a continuous random noise function f and a cutoff value function f_1. The function f defines the size and shape of the phases and the function f_1 defines the probability of finding the material m_1 on a point of the solid. The function f is defined as $f : \mathbb{U}^3 \rightarrow [0,1]$. That is, its domain is the three-dimensional parametric space $\mathbb{U}^3$ and its range is the closed interval $[0,1]$. The cutoff value function f_1 is also defined as $f_1 : \mathbb{U}^3 \rightarrow [0,1]$.

The microstructure of an heterogeneous solid depends on the function f that determines the shape and size of the phases, and on the function f_1 that determines the proportion of each primary material m_i in each area of the solid.

This approach is very flexible, because it allows to design each aspect of the microstructure (shape, size and proportion of the phases) separately and provides great control over the final solid that is being designed.

For a solid made of two primary materials, we use as cutoff value function f_1 the first component of the material distribution function $\mathbf{A}_i(\mathbf{u}) = \mathbf{a} = (a_1, 1-a_1)$, i.e. $f_1(\mathbf{u}) = a_1$. This function is defined in the whole parametric domain $\mathbb{U}^3$ and varies continuously throughout it. This allows us to model phases whose proportion varies continuously within the solid.

In our implementation, we have defined the function f (which defines the location and size of the phases in the solid volume) as a modified version of the periodic Perlin noise function p [Per85]. This function can be evaluated for any point in the parametric domain $\mathbb{U}^3$. Subsection 3.1 gives more details on this topic.

f and f_1 are combined in a function $m(\mathbf{u}), \mathbf{u} \in \mathbb{U}^3$ that is used to compute the phases in the microstructure. This function assigns a

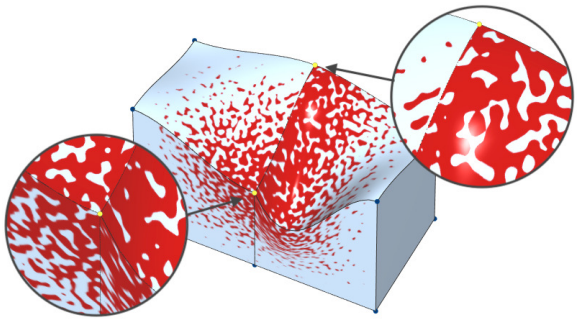

Figure 7: Both C^0 and C^1 continuity can be set independently for each corner point. Also, given a corner point, continuity can be established separately for shape and material distribution. This composite hyperpatch shows C^1 continuity in the material distribution but not in the shape around one corner point (left close-up). At the same time, it shows C^1 continuity in the shape but not in the material distribution around another corner point (right close-up).

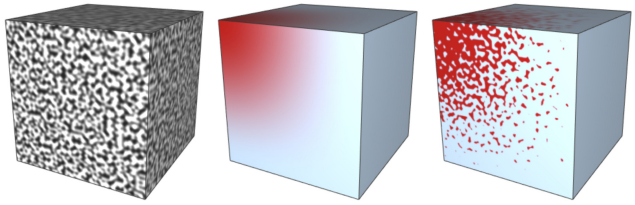

(a) **(b)** **(c)**

Figure 8: Elements involved in microstructure characterization. (a) Uniform normalized Perlin noise function. Values near 0 are depicted in black and values near 1 are depicted in white. This is the random noise function f we use to characterize microstructure. It defines the shape and size of the phases. (b) Material distribution inside the cell. This is the cutoff value function f_1 we use to characterize the volume fraction of each primary material. There are two primary materials: m_1, depicted in red, and m_2, depicted in light grey. At each point $\mathbf{u}$ in the parametric domain of the cell, the material distribution is $\mathbf{A}(\mathbf{u}) = \mathbf{a} = (a_1, 1-a_1)$. The cutoff value function $f_1(\mathbf{u}) = a_1$ represents the proportion of each material at that point. (c) The final microstructure is calculated from the uniform normalized Perlin function by using the value of a_1 at each point as cutoff value. If the value of the uniform normalized Perlin function at a given point $\mathbf{u}$ of the parametric domain of the cell is lower than the value of a_1 at that same point, material m_1 is chosen, and material m_2 is chosen otherwise.

primary material $m_i \in \mathbf{M}$ to every point $\mathbf{u}$ in the parametric domain $\mathbb{U}^3$ of a parametric cell:

$$m(\mathbf{u}) = \begin{cases} m_1 & if \quad f(\mathbf{u}) < f_1(\mathbf{u}) \\ m_2 & if \quad f(\mathbf{u}) \geq f_1(\mathbf{u}) \end{cases} \quad \forall\, \mathbf{u} = (u,v,w) \in \mathbb{U}^3 \qquad (9)$$

Each point $\mathbf{u} = (u,v,w) \in \mathbb{U}^3$ such that $f(\mathbf{u}) < f_1(\mathbf{u})$ is assumed to be occupied by the primary material m_1 and similarly, each point $\mathbf{u} \in \mathbb{U}^3 \mid f(\mathbf{u}) \geq f_1(\mathbf{u})$ is assumed to be occupied by the primary material m_2 (see Figure 8).

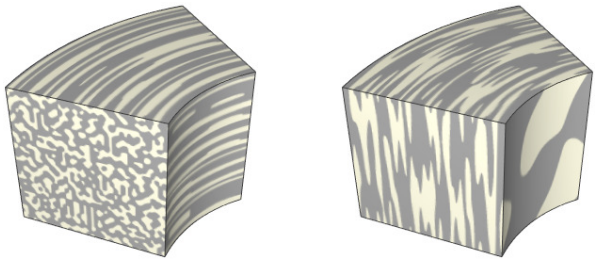

(a) **(b)**

Figure 9: Microstructure with different shapes, sizes and orientations. (a) Fiber-shaped microstructure, obtained by setting $p_u = p_v$, and $p_w << p_u$. (b) Disk-shaped microstructure, obtained by setting $p_v = p_w$, and $p_u >> p_v$.

3.1. Uniform normalized Perlin function

In order to obtain valid material phases susceptible of being manufactured (for example, by means of 3D printing), it is essential for the random function f to be continuous. In order to produce a valid f function, we have implemented a modified version of the 3D periodic Perlin noise function p.

The 3D periodic Perlin noise function p has been widely used in Computer Graphics to generate procedural textures, because it is able to produce a noise component that can be used for simulating natural materials such as marble in a very realistic way. However, in this work we use it as a pseudo-random function that determines how the phases (given a certain shape and size) of an heterogeneous material are distributed throughout a solid volume.

The 3D periodic Perlin noise function [Per85] has six parameters: $p(u',v',w',p_u,p_v,p_w)$, where u',v' and w' are the coordinates of the point for which the function is to be calculated, and p_u, p_v and p_w are the frequencies of the function in each parametric direction. The parameters also verify that $p_u, p_v, p_w \in [2,\infty)$ and $u' \in [0,p_u]$, $v' \in [0,p_v]$ and $w' \in [0,p_w]$.

In our framework, any point $\mathbf{u} = (u,v,w)$ in the parametric domain of a cell $\mathbb{U}^3$ has coordinates $u,v,w \in [0,1]$. As the domain of the coordinates is not equal to the domain of the coordinate parameters of the Perlin function, we have to apply the following transformation: $u' = u\,p_u$, $v' = v\,p_v$ and $w' = w\,p_w$.

For each parametric cell, the Perlin frequencies p_u, p_v and p_w are added as descriptors of the material microstructure of the cell. These parameters determine the amount of material phases over the volume of the parametric cell. A frequency value of 10 means that there will be 10 material phases in that parametric direction within the volume of the parametric cell. Similarly, a frequency value of 100 means that there will be 100 material phases. Note that it is possible to set the frequency values for each parametric direction independently (Figure 9). Moreover, as the frequency values can be set at cell level, it is possible to adjust the continuity of the mi-

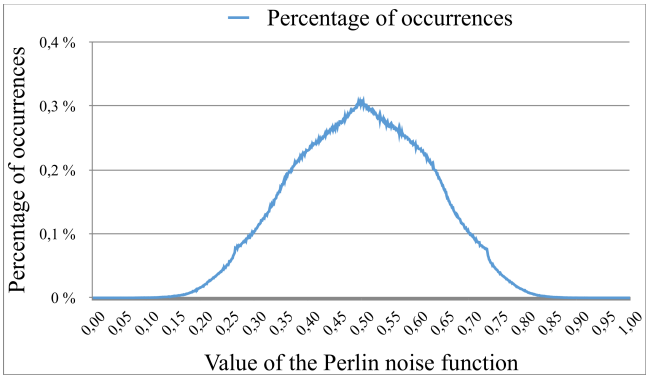

(a)

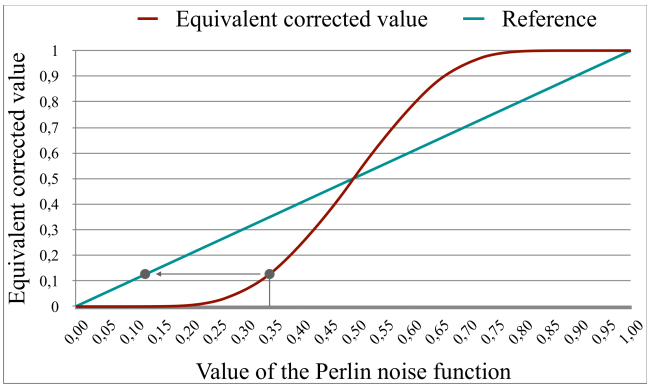

(b)

Figure 10: (a) Histogram of the normalized periodic Perlin noise function. The function has a bias around the value 0.5. (b) In order to remove the bias of the normalized Perlin noise function, the values of the normalized function (in red) are replaced by their uniformized equivalents (in blue), resulting in a uniform distribution of the values in the interval $[0,1]$.

crostructure within the solid volume at will (this will be discussed in detail later).

However, it is necessary to make two minor modifications to the 3D periodic Perlin noise function before using it as our f function, because of the following reasons:

1. The range of the periodic Perlin noise function as defined by its author is the interval $[-1,1]$. As explained above, the range of the function f is the interval $[0,1]$. Therefore, it is necessary to normalize the values produced by p so that they belong to the required range.
2. The distribution of the values produced by the original periodic Perlin noise function is not uniform. In order to produce any value with the same probability, it is necessary to make the values be uniformly distributed along the function range. This process will be described below.

The first issue is easy to resolve. The 3D periodic Perlin noise function produces floating point values in the interval $[-1,1]$. As f is expected to produce values in the interval $[0,1]$, the following normalization has to be applied to the values $np = (p(u',v',w',p_u,p_v,p_w)+1)/2$.

Let us see how to resolve the second issue. The histogram of the normalized periodic Perlin noise function (Figure 10.a) clearly shows that the function is biased around the value 0.5 i.e. the central values of the interval $[0,1]$ (values around 0.5) appear many more times than the external values (values around 0 or around 1).

In practice, this means that the normalized function is more likely to produce values that lie in the center of the interval $[0,1]$, and this makes the volume fraction of each material differ from the one specified by the material distribution (see Figure 11). We solve this problem by using a table of equivalent uniformly distributed values to translate the value produced by the normalized function into a new, uniformized value. The process is as follows:

In order to calculate the uniform normalized periodic Perlin noise value unp, we use an array **unif**. This array is calculated using a three-stage process:

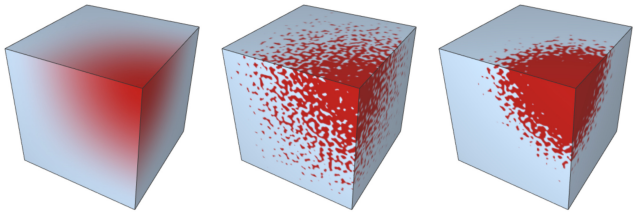

(a) Material distribution **(b)** *unp*. **(c)** *np*.

Figure 11: Effect of using the uniform normalized Perlin noise function unp vs. the normalized Perlin noise function np. Given a material distribution (a), using the uniform normalized Perlin noise function results in a microstructure that correctly reproduces the design (b). In contrast, when only the normalized Perlin is used, the bias around 0.5 cause an abrupt transition between the two phases, and the result does not fit the original design (c).

1. **Count.** Divide the range of the normalized periodic Perlin noise function into a sufficiently large number of intervals ni (in our implementation, $ni = 10^3$) of the same length. Then, evaluate the normalized periodic Perlin noise function a sufficiently large number of times Ns (in our implementation, we use $Ns = 10^6$) and count for each interval how many times the result of the function belongs to it. The output of this stage is an array c of ni elements with the number of occurrences for each interval.
2. **Normalize.** Divide each element of c by Ns to obtain the normalized number of occurrences. Now each element of c belongs to the interval $[0,1]$.
3. **Aggregate**. Calculate the array **unif** of equivalent uniformized values from the values stored in c: the ith element of **unif** is equal to the sum of the first i elements of c. Figure 10.b shows in blue the plot of the values of **unif**.

Note that once the array **unif** of equivalent uniformized values has been computed, it can be saved for future uses, as it does not depend on the function frequencies.

The uniform normalized value of the periodic Perlin noise function is then used for selecting the material at a given point **u** of the parametric domain of a cell with coordinates $u, v, w \in [0,1]$ in the following way:

1. **Generate Perlin noise.** Compute u', v' and w' from u, v and w, and evaluate the 3D periodic Perlin noise function $p(u', v', w', p_u, p_v, p_w)$. Then, apply the normalization to get a value $np \in [0,1]$.
2. **Uniformize.** Compute the interval i to which np belongs ($i = floor(np * ni)$). Then, use the equivalent uniformized value for that interval: $unp =$ **unif**$[i]$. For example, a value of 0.35 is translated into the value 0.1206375 (see Figure 10.b).
3. **Select material.** Once an appropriate Perlin value unp has been obtained, use it as f value in Equation 9, together with the material distribution at **u** to determine the material to be used at that point in the cell.

Algorithm 1 summarizes the process described above.

Algorithm 1 Determine which phase is present at a point **u** of a parametric cell

Input: Parametric coordinates of the point **u** (u, v, w), Perlin frequencies (p_u, p_v, p_w), array of uniformized Perlin values **unif** and material distribution **a** $= (a_1, 1 - a_1)$ at the point **u**
Output: The material (phase value) that best represents the material mixture at the point **u** of the parametric cell

```
                                  { Includes coordinate transformation }
p ← Perlin (u, v, w, p_u, p_v, p_w)
np ← normalizePerlin (p)
i ← floor ( np * unif.size )
unp ← unif[i]
if unp < a_1 then
   pv ← 1                                  { Pick material m_1 }
else
   pv ← 2                                  { Pick material m_2 }
end if
return pv
```

4. Model validation

In order to prove the validity of our framework, we have compared the observed volume fraction of each material inside a number of parametric cells with the modeled material distribution. Our tests confirm that the microstructure produced with our framework successfully mimics the material design, therefore confirming the validity of our proposal. The following paragraphs describe our experiments.

1. For each parametric cell tested, we have generated 2^{10} jittered random points $\mathbf{p}_s \in \mathbb{U}^3$ within the parametric space $\mathbb{U}^3$.
2. For each point $\mathbf{p}_s$ we have defined a random epsilon value $\varepsilon \geq 2/p$, where p is the frequency value of the uniform normalized periodic Perlin noise function unp. For simplicity, we have considered that the same value p was used for the three parametric directions in these tests.
3. Given $\mathbf{p}_s$ and ε, we have considered a spherical neighbourhood centered on $\mathbf{p}_s$ and with radius ε. Then, we have generated 2^{20} sampling points in this neighbourhood, each one with parametric coordinates **u**, and for each of these points, we have computed its material distribution $\mathbf{A}_i(\mathbf{u}) = (a_1, 1 - a_1)$ and its corresponding material (phase value) pv using Algorithm 1.
4. For each parametric cell, we have computed the mean value of a_1 (expected probability of finding material 1, according to the designed material distribution of the cell) at the sample points in the neighbourhood of every $\mathbf{p}_s$, and the observed volume fraction of material 1 through the computed phase values at the same points (this value is computed by adding the occurrences of material 1 in the phase values and dividing the result by the total number of sample points).

Table 1: Summary of the differences between the designed material distribution inside a cell $\overline{a_1}$ and the observed volume fraction of each material obtained by applying our method to calculate microstructure. Each row contains the data of a studied Perlin frequency. The first column indicates the frequency, the second column indicates the mean expected value for material m_1 according to the material distribution, the third column indicates the mean observed value for material m_1 of the microstructure and the fourth column indicates the average of the differences between observed and expected values for that Perlin frequency.

Frequency	$\overline{a_1}$	$\overline{pv}$	$\overline{\lvert a_1 - pv \rvert}$
20	0.547029699	0.544276822	**0.007445180**
40	0.547566887	0.544430949	**0.007042045**
80	0.547705965	0.545294582	**0.005988058**
150	0.547789582	0.544554088	**0.005813939**
300	0.547807896	0.544269652	**0.005982422**
500	0.547758455	0.545274119	**0.006083959**

We have repeated the previously described experiment for different Perlin frequency values and different configurations of material inside the parametric cell. As an example, the results obtained for a given configuration are summarized in Table 1. As can be seen, the difference between the average probability of finding material 1 according to the designed material distribution $\overline{a_1}$ and the observed material 1 volume fraction $\overline{pv}$ is very small. We can therefore ensure that our method generates microstructures that have the same volume fractions of material as the ones designed by the user. The difference does not depend on the Perlin frequency chosen.

We have also modeled examples that mimic real world materials. Figures 12 and 13 show two segmented images of Bentheimer sandstone samples taken from a public CT image repository [JLK19], and our models that mimic their material distribution. As our framework allows interactive modeling, the parameters can be easily adjusted to match the desired requirements.

(a) (b) (c)

Figure 12: Modeling real materials. a) Segmented X-Ray micro-tomography image from steady-state drainage and imbibition flow experiments in Bentheimer sandstone, taken from [JLK19]. b) Modeled hyperpatch that mimics the material distribution of the sample. c) The same hyperpatch, rendered using void as m_2. The material distribution is (0.75, 0.25) over the hyperpatch, and the Perlin frequencies are equal to 16 in the three parametric directions

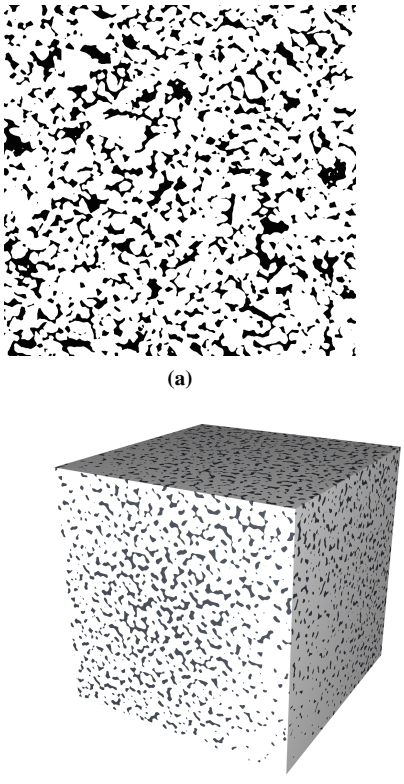

(a) (b)

Figure 13: Modeling real materials. a) Segmented X-Ray micro-tomography image from steady-state drainage and imbibition flow experiments in Bentheimer sandstone, taken from [JLK19]. b) Modeled hyperpatch that mimics the material distribution of the sample. The material distribution varies from (0.7, 0.3) to (1, 0) over the hyperpatch, and the Perlin frequencies are equal to 21 in the three parametric directions

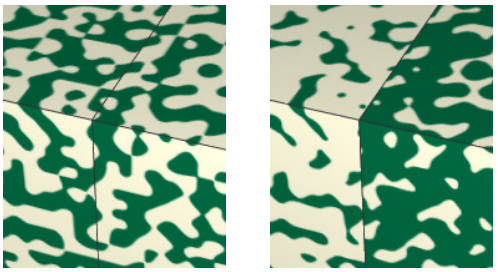

(a) (b)

Figure 14: Continuity on the microstructure over cell joints occurs naturally (a), just by assigning the same values of the material distribution and the Perlin parameters to the corner points of adjacent cells. However, it is also possible to control the continuity level in isolation at every interface between cells by just changing these parameters on the corner points of each cell. Note that the continuity in material distribution and the geometric continuity can be adjusted independently. (a) Adjacent cells with continuous material distribution. (b) Adjacent cells with discontinuity in the material distribution.

5. Results

The proposed model can ensure continuity on the shape, size and orientation of the different phases across the cell boundaries.

As shown in section 3, the shape and size of each phase within a parametric cell depend on the periodic Perlin noise function and the material distribution in that cell. Both functions have been specifically designed to be continuous across adjacent cells, and therefore, the phases that lie in the boundary of two cells spread continuously across them, without requiring any special care from the designer of the solid (Figure 14.a).

Delving into continuity, our model allows to directly choose be-

tween C^0 or C^1 shape continuity across the parametric cell joints, as explained above. Moreover, it also allows to handle material continuity, since the shape and size of each material phase within a parametric cell depends on the uniform normalized periodic Perlin noise function and the material distribution of the cell, and both functions can be continous across adjacent cells, just by assigning the same parameters to the corner points of the adjacent cells (Figure 14.a). In contrast, if no material continuity is necessary, it is also possible to model material discontinuities by changing either the Perlin parameters or the material distribution, as shown in Figure 14.b.

The shape, size, and volume fraction of the phases within a cell is not bound to the position or orientation that the cell occupies in three-dimensional space $\mathbb{R}^3$, but to its parametric domain $\mathbb{U}^3$. This is because the interpolated values for the material distribution along each parametric cell and the periodic Perlin noise function at each point inside each parametric cell of the solid are a function of the parametric coordinate space of that cell $\mathbb{U}^3$ (see Section 2). They are not a function of the actual coordinates of the points in the three-dimensional space.

This fact provides us with a great advantage when working with heterogeneous solids based on our Heterogeneous Composite Bézier hiperpatches: the generated microstructure always follows the shape in 3D space of the modeled solid, while preserving the volume fraction of the materials. For example, if the solid is compressed its internal microstructure will also be compressed, just as it happens in a real solid (Figure 15.a). Similarly, a bending deformation applied to a set of cells also deforms the inner microstructure, following the geometry of the cells (Figure 15.b). The microstructure adapts to the shape of the modeled solid like real solids do. This allows us to simulate fabrication processes such as folding easily.

However, it is also possible to adjust the frequencies of the Perlin noise function to compensate the microstructure deformation, if needed (Figure 15.c).

The material microstructure can be modeled at different scales depending on the specific fabrication process that we want to reproduce or simulate (see Figure 16). We can achieve this by adjusting the frequencies of the periodic Perlin noise function.

Additionally, it is possible to define a different scale for each direction of the parametric space $\mathbb{U}^3$ by setting the proper values of the Perlin frequencies. This produces phases whose shape is similar to spheres, fibers or disks with different sizes (see Figure 9). As a result, the framework allows to model solids that are statistically homogeneous or isotropic, as well as solids that are statistically anisotropic. This is very interesting, since the properties of a particular composite material depend not only on the volume fraction of each primary material, but also on microstructural information such as shape or orientation of the phases. The ability of a framework to precisely model such microstructural information is very important (Figure 17).

6. Discussion and conclusions

We have summarized how our framework based on heterogeneous composite Bézier hyperpatches allows us to represent in a compact way complex heterogeneous solids and edit them interactively using a simple and intuitive mechanism [CTGF15]. This is done by associating material distribution coefficients to the corner points of each parametric cell and using the Bézier interpolation function to compute the material distribution throughout the volume of each cell (Figure 18).

In this paper we have presented a method to represent the microstructure of the solid by using a modified version of the periodic Perlin noise function to associate primary materials at local level. Other authors use a different function which is expressed in terms of a combination of Gaussian functions [Tor02, VG10]. We have chosen the periodic Perlin noise function because it has several advantages:

- It is inherently periodic, therefore it is not necessary to evaluate special cases in order to create a locally periodic microstructure with continuous material interfaces across the cell boundaries.
- It is possible to define the size of the phases relative to the size of the solid domain $\mathbb{U}^3$ of each cell. To do this, it is only necessary to adjust the frequencies of the periodic Perlin noise function. This allows us to model phases at different scales, from microns to meters.
- It is also possible to model phases with different shapes. For example, if we use the same value for the three frequencies, we obtain phases whose shape is similar to a sphere. If we use the same value for two of the three frequencies and a smaller value for the third, we obtain phases whose shape is similar to a disc, and so on. Using our method we can model a great variety of phase shapes.

Previous approaches worked with a B-rep representation of the solid, defining the material distribution in the modeling space. This makes it difficult to deform the represented solid while maintaining the microstructure (for instance bending it). Our approach takes advantage of defining the material distribution on the parametric space $\mathbb{U}^3$, allowing us to carry out any deformation of the solid easily.

The proposed approach guarantees that the locally generated material fraction corresponds with the one computed using the Bézier interpolation function. It may also ensure the continuity of the different phases across the cell boundaries.

The framework allows to model complex solids in a simple and efficient way. However, it is still possible to extend it further. At this moment, we are developing algorithms to compute Boolean operations based on our framework, which would allow us to model operations such as machining mechanical parts in a simple way.

Acknowledgements

This work has been partially funded by the Spanish Ministry of Economy and Competitiveness through grants TIN2017-85259-R and TIN2017-84968-R with ERDF funds.

References

[ABC*19] ANTOLIN P., BUFFA A., COHEN E., DANNENHOFFER J. F., ELBER G., ELGETI S., HAIMES R., RIESENFELD R.: Optimizing Micro-Tiles in Micro-Structures as a Design Paradigm. *Computer-Aided*

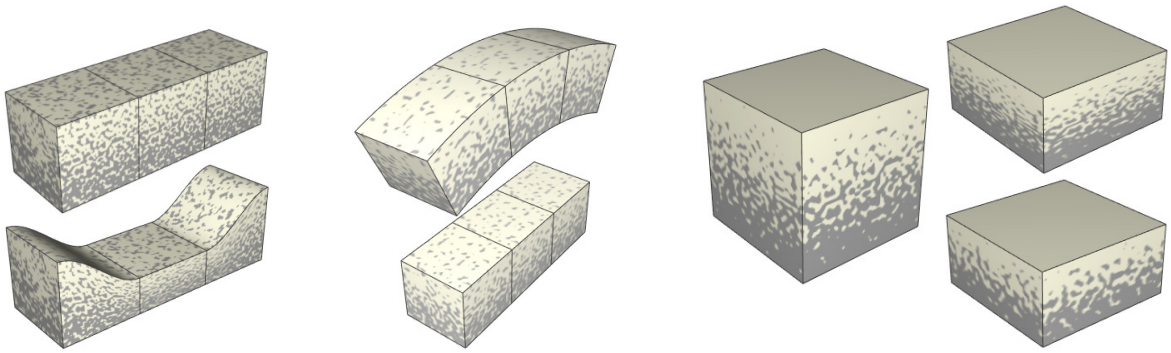

(a) Original bar (top) and after compression (bottom). The microstructure is also compressed.

(b) Original bar (bottom) and after bending (top). The microstructure is also bent following the geometry of the bar.

(c) Original parametric cell (left) and after shrinking (right). On top, the microstructure is also shrunk. At the bottom, the microstructure parameters have been modified, so that it retains its aspect.

Figure 15: The microstructure of the solids adapts to their shape after modeling operations. This allows us to simulate manufacturing processes such as shrinking, folding or bending in a very easy way.

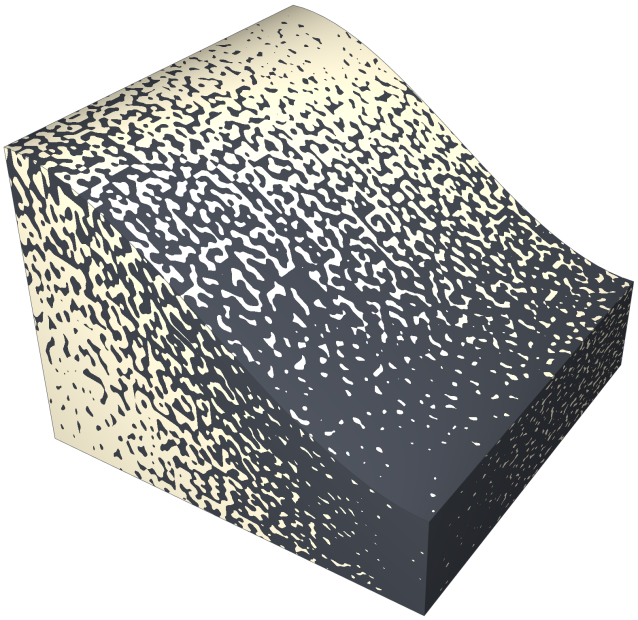

Figure 17: Parametric cell with variable material microstructure. The material distribution changes over the volume from (1, 0) on the top back corner to (0, 1) on the bottom front corner; on the left side, the material distribution varies from (0.5, 0.5) at the top, and (1, 0) at the bottom, while on the right side, the material distribution is (0.2, 0.8).The Perlin frequencies are $p_u = 51$, $p_v = 25$ and $p_w = 51$.

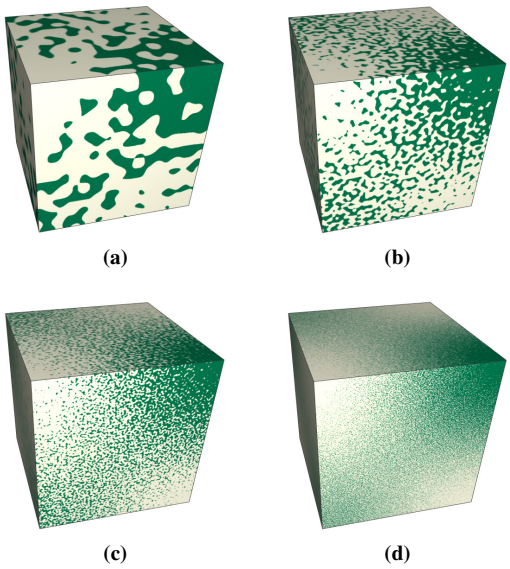

Figure 16: Microstructure representing the same material distribution modeled at different scales. (a) Very large scale. (b) Large scale. (c) Medium scale. (d) Small scale.

Design 115 (Oct. 2019), 23–33. doi:10.1016/j.cad.2019.05.020. 2

[BB07] BIRMAN V., BYRD L. W.: Modeling and analysis of functionally graded materials and structures. *Applied Mechanics Reviews 60*, 5 (Sept. 2007), 195–216. doi:10.1115/1.2777164. 1

[BZL*18] BOSTANABAD R., ZHANG Y., LI X., KEARNEY T., BRINSON L. C., APLEY D. W., LIU W. K., CHEN W.: Computational microstructure characterization and reconstruction: Review of the state-of-the-art techniques. *Progress in Materials Science 95* (June 2018), 1–41. doi:10.1016/j.pmatsci.2018.01.005. 2

[CRGFT20] CONDE-RODRÃ■GUEZ F., GARCÃ■A-FERNÃ‚NDEZ Á.-L., TORRES J.: Modeling the Internal Architecture of Composites. *Computer-Aided Design 129* (Dec. 2020), 102930. doi:10.1016/j.cad.2020.102930. 2

[CRTC01] CONDE RODRIGUEZ F. D. A., TORRES CANTERO J. C.: A Simple Validity Condition for B-Spline Hyperpatches. In *Eurographics*

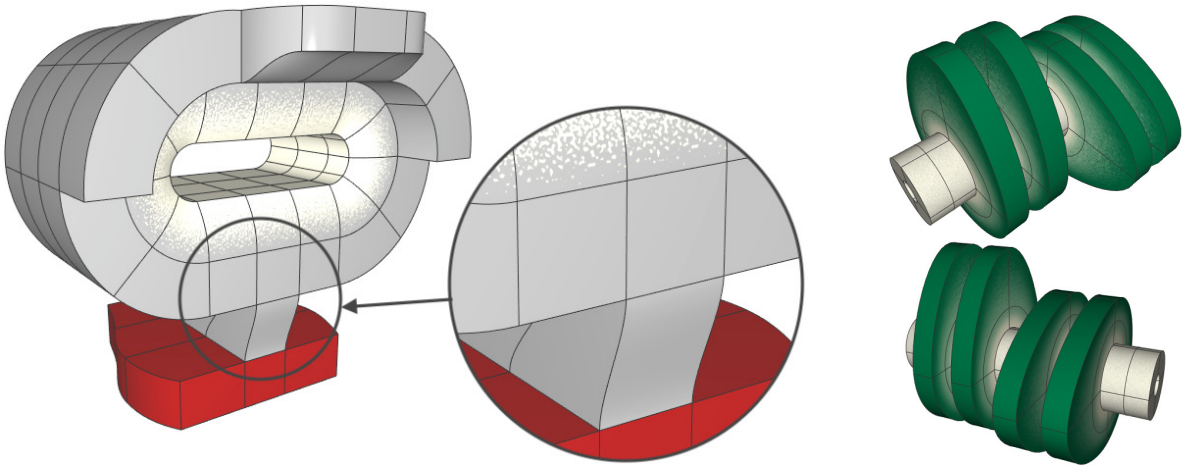

(a) (b)

Figure 18: Heterogeneous mechanical parts modeled with our framework. They have three primary materials and microstructure. It can be seen that although inside each cell there are only one or two materials, the total number of materials that can be used in the whole solid is unlimited. (a) Our framework allows us to model continuous or discontinuous transitions in the microstructure between cells. (b) Two views of a camshaft.

2001 - Short Presentations (Manchester, UK, 2001). doi:10.2312/egs.20011010. 4

[CRTGFFH17] CONDE-RODRÍGUEZ F., TORRES J.-C., GARCÍA-FERNÁNDEZ Á.-L., FEITO-HIGUERUELA F.-R.: A comprehensive framework for modeling heterogeneous objects. *Vis. Comput. 33*, 1 (Jan. 2017), 17–31. doi:10.1007/s00371-015-1149-0. 2

[CTGF15] CONDE F., TORRES J. C., GARCÍA Á. L., FEITO F.: Heterogeneous object modeling. In *Proceedings of 32nd Computer Graphics International. Full papers* (Strasbourg, France, June 2015), CGI. 2, 3, 11

[Elb17] ELBER G.: *Precise construction of micro-structures and porous geometry via functional composition*, vol. 10521 LNCS of *Lecture Notes in Computer Science (including subseries Lecture Notes in Artificial Intelligence and Lecture Notes in Bioinformatics)*. Springer, 2017. doi:10.1007/978-3-319-67885-6_6. 2

[GAR18] GUPTA A., ALLEN G., ROSSIGNAC J.: QUADOR: QUADric-Of-Revolution beams for lattices. *Computer-Aided Design 102* (Sept. 2018), 160–170. doi:10.1016/j.cad.2018.04.015. 2

[GV10] GOUPEE A. J., VEL S. S.: Multiscale thermoelastic analysis of random heterogeneous materials. part ii: Direct micromechanical failure analysis and multiscale simulations. *Computational Materials Science 48*, 1 (2010), 39–53. doi:10.1016/j.commatsci.2009.10.004. 3

[JA06] JONES D. R., ASHBY M. F.: *Engineering materials 2: an introduction to microstructures, processing and design*. Butterworth-Heinemann, Oxford, UK, 2006. 1

[JLK19] JACKSON S., LIN Q., KREVOR S.: A large scale x-ray microtomography dataset of steady-state multiphase flow, 2019. doi:10.17612/KT0B-SZ28. 9, 10

[LS15] LIU X., SHAPIRO V.: Random heterogeneous materials via texture synthesis. *Computational Materials Science 99* (Mar. 2015), 177–189. doi:10.1016/j.commatsci.2014.12.017. 2

[LS18] LIU X., SHAPIRO V.: Multiscale shapeâĂŞmaterial modeling by composition. *Computer-Aided Design 102* (Sept. 2018), 194–203. doi:10.1016/j.cad.2018.04.024. 3

[MDL16] MARTÍNEZ J., DUMAS J., LEFEBVRE S.: Procedural voronoi foams for additive manufacturing. *ACM Trans. Graph. 35*, 4 (July 2016). doi:10.1145/2897824.2925922. 3

[ME16] MASSARWI F., ELBER G.: A B-spline based framework for volumetric object modeling. *Computer-Aided Design 78* (Sept. 2016), 36–47. doi:10.1016/j.cad.2016.05.003. 2

[Mor85] MORTENSON M. E.: *Geometric Modeling*. John Wiley & Sons, Inc., New York, NY, USA, 1985. 5

[Per85] PERLIN K.: An image synthesizer. *SIGGRAPH Comput. Graph. 19*, 3 (July 1985), 287âĂŞ296. doi:10.1145/325165.325247. 6, 7

[PFV*11] PASKO A., FRYAZINOV O., VILBRANDT T., FAYOLLE P.-A., ADZHIEV V.: Procedural function-based modelling of volumetric microstructures. *Graphical Models 73*, 5 (2011), 165 – 181. doi:10.1016/j.gmod.2011.03.001. 3

[RRSS16] REGLI W., ROSSIGNAC J., SHAPIRO V., SRINIVASAN V.: The new frontiers in computational modeling of material structures. *Comput.-Aided Des. 77* (Aug. 2016), 73–85. doi:10.1016/j.cad.2016.03.002. 2

[RT95] ROBERTS A. P., TEUBNER M.: Transport properties of heterogeneous materials derived from gaussian random fields: Bounds and simulation. *Phys. Rev. E 51* (May 1995), 4141–4154. doi:10.1103/PhysRevE.51.4141. 3

[SPS04] SCHMITT B., PASKO A., SCHLICK C.: Constructive sculpting of heterogeneous volumetric objects using trivariate B-splines. *The Visual Computer 20*, 2 (May 2004), 130–148. doi:10.1007/s00371-003-0236-9. 3

[ST02] SIU Y. K., TAN S. T.: Modeling the material grading and structures of heterogeneous objects for layered manufacturing. *Computer-Aided Design 34*, 10 (2002), 705–716. doi:10.1016/S0010-4485(01)00200-7. 2

[Tor02] TORQUATO S.: *Random heterogeneous materials: microstructure and macroscopic properties*, vol. v. 16. Springer, New York, USA, 2002. 1, 11

[VCJG16] VEL S., COOK A., JOHNSON S., GERBI C.: Computational homogenization and micromechanical analysis of textured polycrystalline materials. *Computer Methods in Applied Mechanics and Engineering 310* (2016), 749–779. doi:10.1016/j.cma.2016.07.037. 3

[VG10] VEL S. S., GOUPEE A. J.: Multiscale thermoelastic analysis of random heterogeneous materials. part i: Microstructure characterization and homogenization of material properties. *Computational Materials Science 48*, 1 (2010), 22–38. doi:10.1016/j.commatsci.2009.11.015. 3, 11

[Wor96] WORLEY S.: A cellular texture basis function. In *Proceedings of the 23rd annual conference on Computer graphics and interactive techniques* (New York, NY, USA, Aug. 1996), SIGGRAPH '96, Association for Computing Machinery, pp. 291–294. doi:10.1145/237170.237267. 3

[WWG19] WU J., WANG W., GAO X.: Design and Optimization of Conforming Lattice Structures. *IEEE Transactions on Visualization and Computer Graphics* (2019), 1–1. doi:10.1109/TVCG.2019.2938946. 2

[XDBC14] XU H., DIKIN D. A., BURKHART C., CHEN W.: Descriptor-based methodology for statistical characterization and 3D reconstruction of microstructural materials. *Computational Materials Science 85* (Apr. 2014), 206–216. doi:10.1016/j.commatsci.2013.12.046. 2

[YNLS18] YANG M., NAGARAJAN A., LIANG B., SOGHRATI S.: New algorithms for virtual reconstruction of heterogeneous microstructures. *Computer Methods in Applied Mechanics and Engineering 338* (Aug. 2018), 275–298. doi:10.1016/j.cma.2018.04.030. 3

[ZSCM17] ZHU B., SKOURAS M., CHEN D., MATUSIK W.: Two-Scale Topology Optimization with Microstructures. *ACM Transactions on Graphics 36*, 5 (July 2017). doi:10.1145/3095815. 2